Multi-Chirp Piecewise Linearly Frequency Modulated Microwave Generation Using a Semiconductor Laser

Bikash Nakarmi, *Senior Member, IEEE*, Bai Yan Song, Hum Nath Parajuli, Ikechi Augustine Ukaegbu, *Senior Member, IEEE*, Wang Xiangchun, *Member, IEEE*, and Shilong Pan, *Fellow, IEEE*

***Abstract*— A simple structured photonics-based multi-chirp piecewise linearly frequency modulated microwave (Ph-MPLFM) waveform is proposed and demonstrated experimentally for radar systems. The proposed technique consists of a main laser which is injected into a typical secondary laser, distributed feedback (DFB) laser, with a negative wavelength detuning for the radio frequency (RF) signal generation. The frequency of the generated RF signal is varied by implementing the redshift phenomenon in the emission wavelength of the secondary laser. We introduced a series of piecewise arbitrary waveform with different amplitude-time slopes to obtain the controlled redshift of an emission wavelength of a DFB laser. In this work, two- and three-chirp LFM waveforms are demonstrated. The generated Ph-MPLFMs have a total time period of 1 μs with equal sub-interval periods. The generated two-chirp Ph-MPLFM has chirp rates of 6 GHz/μs and 10 GHz/μs. The chirp rate and the number of chirps can be reconfigured by modifying the applied piecewise arbitrary wave generator (AWG) signal to the intensity modulator. As part of reconfigurability, two and three-chirp PH-MPLFMs with different chirp rates, 3 GHz/us, 15 GHz/us, and 3 GHz/us; and 6 GHz/μs, 15 GHz/μs, and 3 GHz/μs are demonstrated. The generated Ph-MPLFM has the FWHM and Doppler resolution of 120 ps and 0.7 MHz for three-chirp waveforms. Hence, the proposed Ph-MPLFM radar waveform can be used as a promising and robust radar waveform in multi-radar environment applications.**

***Index Terms*— Multi-chirp LFM, photonic signal generation, photonics radar, multi-radar environment, semiconductor lasers.**

I. Introduction

PHOTONICS based radars have been of great interest due to their inherent advantages over their electronic counterparts in terms of bandwidth, electromagnetic immunity, all-weather capability, and better signal processing techniques [1]. Various transmission waveforms such as continuous, pulse, triangular, linearly frequency modulated (LFM) and others have been investigated for radar purposes [2]. Among these, LFM is a widely used waveform due to its numerous advantages such as high pulse compression ratio, long detection range, and better range resolution. One of these techniques relies on the baseband waveform and the dual-band, higher-order electro-optic modulator [3]. Others rely on the optoelectronic oscillator which uses highly stable notch filter and phase modulator [4]. However, these techniques are complex in structure, and have achieved only a single chirp signal. Few researchers have focused on the use of optical injection technology to generate the LFM signal by utilizing the redshift phenomena in a semiconductor laser [5], [6]. The optical injection technology is simple in structure, flexible in reconfiguration, and provides a high bandwidth of LFM signal. Using optical injection technology, LFM and dual-band LFM signals with identical and complementary LFM signals have been demonstrated in our previous research [7], which can be used for the photonics-based radar system for reducing the delay-Doppler coupling effect and improving range velocity resolution [8].

These techniques of generating photonics-based waveforms mainly focus on improving the resolution and efficiency of radars [3], [5], [7], [8] and have not taken consideration of the safety issues due to interferences. With an increase in the number of radar users, radars are more prone to interferences and intruders. Therefore, there is no guarantee of their secure and error-free detection. Also, disturbances such as spoofing and jamming have become critical issues and hence, need to be resolved [9]. The most prominent and usual case of disturbance is mutual interference when multiple radars are working in the same environment which can degrade the effectiveness of a radar. Also, the intentional adversaries' disturbing and impeding techniques to diminish the effectiveness of radar become a usual case, which falls under spoofing in a multi-radar environment. In both cases of mutual interference and spoofing, the Ph-LFM signal cannot meet the requirement of safe and secure operation, thus, affecting the signal-to-noise ratio (SNR) and introducing a ghost signal to the radar [10]. To mitigate the interference and disruptions in the multi-radar scenarios, several techniques have been used, such as

Manuscript received 5 April 2023; revised 25 May 2023; accepted 27 May 2023. Date of publication 31 May 2023; date of current version 16 June 2023. This work was supported in part by the Nanjing University of Aeronautics and Astronautics Collaborative Research under Grant 1004-KFA22645, in part by Nazarbayev University Collaborative Research under Grant 11022021CRP1507, and in part by the Ministry of Education and Science of the Republic of Kazakhstan under Grant AP14871109. *(Corresponding authors: Bikash Nakarmi; Shilong Pan.)*

Bikash Nakarmi, Bai Yan Song, Wang Xiangchun, and Shilong Pan are with the Key Laboratory of Radar Imaging and Microwave Photonics, Ministry of Education, Nanjing University of Aeronautics and Astronautics, Nanjing 210016, China (e-mail: bikash@nuaa.edu.cn; pans@nuaa.edu.cn).

Hum Nath Parajuli and Ikechi Augustine Ukaegbu are with the Integrated Device Solutions and Nanophotonics (iDSN) Laboratory, Department of Electrical and Computer Engineering, School of Engineering and Digital Sciences, Nazarbayev University, 010000 Astana, Kazakhstan (e-mail: ikechi.ukaegbu@nu.edu.kz).

Color versions of one or more figures in this letter are available at https://doi.org/10.1109/LPT.2023.3281640.

Digital Object Identifier 10.1109/LPT.2023.3281640

changing the transmission signal by developing less detectable waveforms [11], multiband operation [12], more robust waveforms [13], reconstructing and canceling the interference in the receiver unit [14], wavelet denoising [15], and many others. The MOSARIM research project [16] indicates that the potential factors for mitigating the interference effect can be classified into six domains: polarization, time, frequency, space, coding techniques and adaptive methods. Among these, the frequency domain and adaptive techniques are most impressive in mitigating interference. The generation of a robust waveform has provided wide possibilities for mitigating interference. The generation of different types of waveforms including step frequency hopping, continuous frequency signal and the complementary chirp LFM signals are presented in our previous demonstrations [7], [17], [18] but were limited to a single chirp rate LFM generation. Mitigating interference using a single chirp LFM is not well suited without employing advanced signal processing techniques. Therefore, multiple chirp rate sequence-based signals are seen as potential candidates for overcoming interference in a multi-radar environment [19].

In this letter, considering interference and its impact on the radar safety and security, we propose and experimentally demonstrate a photonically generated robust waveform that has multiple chirps within the same time interval, namely, a multi-chirp piecewise linear frequency modulated microwave (Ph-MPLFM), using a single beam injection in a semiconductor (DFB) laser. Under the injection of the external beam, the redshift in the emission frequency of the secondary laser (SL) can be obtained and on optical to electrical conversion, the microwave signals with different frequencies can be generated [6]. By generating the AWG waveform with different amplitude-time slope within the subinterval, the controlled redshift in the emission of the semiconductor laser can be obtained, as a result, a multi-chirp LFM signal with different chirp rates can be generated. For the proof-of-concept demonstration, we have generated two- and three-chirp piecewise LFM signals within the time interval of 1 μs. The auto-ambiguity function is used to calculate the range-doppler resolution of the generated waveforms. Furthermore, this technique provides flexibility in changing the chirp rates and the number of chirps by changing the AWG waveform. Therefore, the proposed scheme is simple in structure, easy to reconfigure the parameters of output waveform, and low cost, which can be promising for the radars operating in the multi-radar environment.

II. Experimental Setup

The experimental setup of the proposed Ph-MPLFM waveform based on single beam injection into a semiconductor laser is shown in Fig.1. For the demonstration, we used a distributed feedback laser (DFB), (Actech LD15DM), which is operated with a bias current of 17mA at a temperature of 23.7°C. The temperature of the SL is stabilized through the temperature controller (Thorlabs TED 200C), which has a resolution of 0.01 °C with temperature stability of ≤0.002 °C (for 24 hours). The DFB output power is controlled through

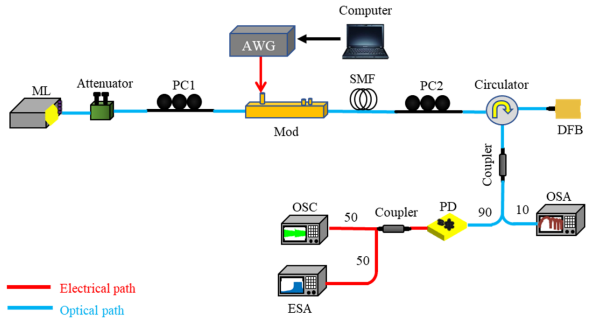

Fig. 1. Experimental set-up of the proposed Ph-MPLFM waveform with a single beam injection into a semiconductor laser.

the low noise (<0.2 μA) laser driving controller (Thorlabs LDC 205C), which has 10 μA resolution. Under these biasing conditions, the DFB laser has an emission wavelength of 1541.96 nm with an output power of −9.7 dBm. One port of the Agilent N7714A tunable laser, which has a wavelength and power tuning range of 1535 nm to 1565 nm and 5 dBm to 16 dBm, respectively, is used as the ML. The ML is set at a wavelength of 1541.89 nm and the power is varied from 11 dBm to 16 dBm. The optical attenuator is used to control the optical power of the injected ML beam. The polarization controllers, PC1 and PC2, are used to control the polarization of the ML so that low loss is maintained in the polarization-dependent Mach-Zehnder modulator, MZM, (Lucent 2623NA), and only TE polarized light is injected to the SL. The 120 MHz baseband AWG (Agilent 81150A) generated signal is used to modulate the power of the ML through an MZM. The output of the SL through the circulator is divided into two parts through a 90:10 coupler. The 10% of the optical output is used for analyzing the output signal through an optical spectrum analyzer (OSA, Yokogawa AQ6370C) whereas the 90% of the output from the SL is sent to a PD, (u2t XPDV2120RA), which has a 3-dB bandwidth of 40 GHz, for optical to electrical conversion. Furthermore, the microwave signal generated through the optical beating in the PD is analyzed through an electrical oscilloscope (OSC, Keysight DSO-X 92504A) and an electrical spectral analyzer (Agilent E447A).

III. Operating Principle and Results

A. Operating Principle

The basic principle of the proposed scheme is the change in rate of the redshift of the emission wavelength of the SL depending upon the applied modulating signal through the AWG. Fig. 2 illustrates the optical and electrical spectrum of the SL without and with the injection of the ML with a constant wavelength detuning of 0.07 nm. Fig. 2(a) shows the optical spectrum at the output of the SL just after the circulator. The dotted line indicates the spectrum of the DFB laser without the injection of the ML whereas the solid line indicates the output spectrum after the injection of the ML with a power of 15 dBm. With the injection of ML, we observed the redshift of the emission wavelength of the SL, and an RF signal of 16.2 GHz is obtained through an optical beating in PD, which is shown in Fig. 2(b). On changing the power of the

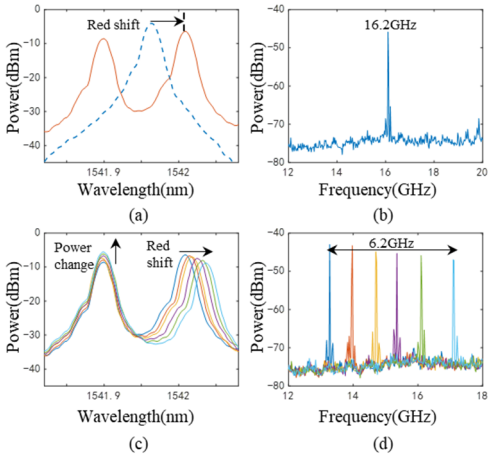

Fig. 2. Redshift in a semiconductor laser diode with an injection of the external beam. (a) Optical spectrum at the output of a DFB laser without (dotted line) and with an injection of ML (solid line), (b) electrical spectra after the PD, (c) redshift phenomena and (d) Electrical spectrum corresponding to (c).

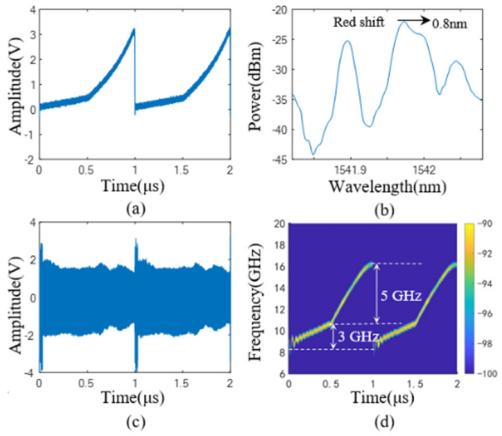

Fig. 3. Two-chirps piecewise LFM signal. (a) Amplitude-time diagram of the control signal, (b) optical output of SL, (c) amplitude-time diagram at the output, and (d) instantaneous time-frequency diagram.

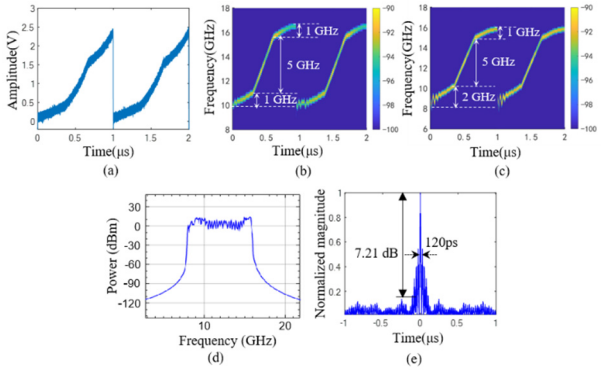

Fig. 4. Reconfigurability of the proposed scheme (a) Control signal for three chirps, (b) corresponding frequency-time diagram of (a), (c) frequency-time diagrams of three chirps with different chirp rate and starting frequencies, (d) offline generated spectrum of the generated three chirp signal, and, (e) autocorrelation function corresponding to (c).

injected ML using an attenuator, the redshift of the emission wavelength of the SL changes. Figure 2(c) shows the optical spectra showing the change in the redshift from 1542.00 nm to 1542.03 nm with a change in the ML's power from 11 dBm to 16 dBm. The corresponding shift in the electrical domain after optical-to-electric conversion is shown in Fig. 2(d) that generates signals with the frequencies from 13.27 GHz to 17.11 GHz at the output. The observation in Fig.2 confirms that the redshift can be controlled by controlling the intensity of the injected ML. Hence, by applying a different amplitude-time slope control signal, the rate of redshift can be controlled, which further provides different chirp-rate LFM waveforms in our experiment. While implementing different amplitude-time slope control signal, one must ensure that there is no overlap and gap at the output and consider the phase fluctuations caused by the change in the amplitude-time slope within the same time-interval.

B. Results

The analysis in Section III-A is used to design the modulating signal (AWG signal) that modulates the intensity of the ML using the intensity modulator, which is further injected into the SL. For the proof-of-demonstration experiment, a total bandwidth of 8 GHz, which is obtained through the redshift, is divided into two and three equal subintervals. Each subinterval is modulated with the almost linear AWG waveform with different amplitude-time slopes. The almost linear AWG waveform, instead of linear AWG, is used to compensate the non-linearity redshift due to the non-linear dynamics of the semiconductor laser. As a result, LFM signals of different chirp rates can be generated. The AWG signal with two different amplitude-time slopes for generating two chirps piecewise linear LFM is shown in Fig. 3(a), while the optical output of the SL with the AWG signal is shown in Fig. 3(b). The amplitude-time diagram of the AWG signal shows that the amplitude of 0 to 3.2 V AWG signal is divided into 0 V to 0.5 V and 0.5V to 3.2V for subinterval 1 and subinterval 2, respectively. Since the subinterval time is same but the amplitude variation within the subinterval is different, i.e., 0.5 V and 2.7 V, the rate of shift of the emission wavelength will be different for each sub-interval. As a result, the two-chirp rate signals of 6 GHz/us and 10 GHz/us are observed at the output. The amplitude-time diagram of the generated two chirps piecewise linear LFM signal is shown in Fig. 3(c) whereas the frequency-time diagram is shown in Fig. 3(d).

Further, to show the flexibility of the proposed technique in terms of the chirp rate, the number of chirps, and the operating frequency range, three-chirp piecewise LFM signals are generated as shown in Fig.4. Fig. 4(a) shows the amplitude-time diagram of the control signal from the AWG, which ranges from 0 to 2.3 V and divided into three equal subintervals with amplitude ranges from 0.3 V (0 - 0.3), 1.4 V (0.3 - 1.7), and 0.6 V (1.7 - 2.3) providing different amplitude-time slopes. Fig. 4(b) shows the frequency-time diagram of the three-chirp signal with chirp rates of 3 GHz/us, 15 GHz/us, and 3 GHz/us, and the starting-stopping frequency from 10 - 11 GHz, 11 - 16 GHz, and 16 - 17 GHz, respectively, with equal subinterval time of 0.33 us. The change in the initial frequency of the Ph-MPLFM can be changed by changing the wavelength detuning. The change in the wavelength detuning can be

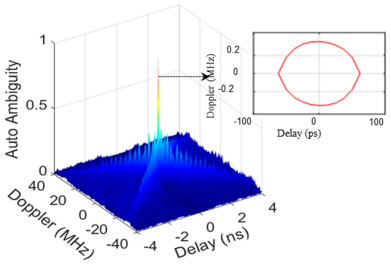

Fig. 5. The normalized auto-ambiguity function of the generated three chirps Ph-MPLFM. Inset: the 3-dB contour map of the auto-ambiguity function.

obtained by changing the wavelength of the ML, however, it requires the modification in the AWG amplitudes range. It should also be noted that since the range of applied AWG voltage in Fig. 4(a) is less than that in Fig.3 (a), a 1 GHz bandwidth decrease is observed. This is because the redshift of the emission wavelength is dependent on the intensity of the ML. Figure 4(c) shows the three-chirps LFM signal with different chirp rates, 6 GHz/us, 15 GHz/us, and 3 GHz/us, which illustrates the reconfigurability of chirp rates, starting frequencies, and the number of chirps. Fig. 4(d) and (e), respectively, show the offline generated RF spectrum of the captured signal from the oscilloscope and the autocorrelation function of the generated Ph-MPLFM. From the autocorrelation function, full-width half maximum (FWHM) of 120 ps providing the pulse compression ratio of 8333.33 and peak to side lobe ratio of 7.2 dB are obtained.

Next, the auto-ambiguity function of the generated Ph-MPLFM signals is investigated as a matched filter response for analyzing the delay and Doppler resolution. The nonzero values of the time delay and Doppler shift variables in the auto-ambiguity function gives the mismatches in the delay and Doppler shift, compared to the transmitted signal. The normalized ambiguity function of a three-chirp signal is shown in Fig. 5, where the main lobe is observed at the origin. The -3dB contour map of the main lobe is shown in the inset. It has been observed that the minor side lobes for the two- and three-chirp Ph-MPLFM waveforms are seemingly decreasing whereas the main lobe is compressed in the time domain and its amplitude is increased, resulting in an amplitude-enhanced narrow peak. From the calculation, a delay of 120 ps is obtained at FWHM. Similarly, a Doppler resolution of 0.7 MHz is observed.

IV. Conclusion

In conclusion, we have proposed and demonstrated a Ph-MPLFM waveform with an injection of a single beam in the semiconductor laser. In the experiment, we modulate the intensity of the injected beam with the different amplitude-time slope AWG waveform within the total time interval to control the rate of the redshift of the emission wavelength of the SL in subintervals. While implementing different amplitude-time slopes control signal, overlapping and gaps should not be observed in the output multi-chirp LFM signal. Also phase changes and the fluctuations in the output frequency should be considered while designing the control signal. As a proof-of-concept demonstration, two- and three-chirp LFM signal is demonstrated. The flexibility in the chirp rate, number of chirps, starting frequency, and bandwidth is demonstrated through the three-chirp Ph-MPLFM. The auto-correlation function and the auto-ambiguity function confirm the performance of the proposed technique. The flexibility of changing the parameters and the large compression ratio of the demonstrated Ph-MPLFM assures its application in modern radar systems, including interference mitigation techniques.

References

[1] G. Sun, F. Zhang, B. Gao, Y. Zhou, Y. Xiang, and S. Pan, "Photonics-based 3D radar imaging with CNN-assisted fast and noise-resistant image construction," *Opt. Exp.*, vol. 29, no. 13, pp. 19352–19361, 2021.

[2] A. M. Richards, "Radar waveforms," in *Fundamentals of Radar Signal Processing*, 2nd ed. New York, NY, USA: McGraw-Hill, 2014.

[3] Z. Meng et al., "Dual-band dechirping LFMCW radar receiver with high image rejection using microwave photonic I/Q mixer," *Opt. Exp.*, vol. 25, no. 18, pp. 22055–22065, Sep. 2017.

[4] T. Hao et al., "Breaking the limitation of mode building time in an optoelectronic oscillator," *Nature Commun.*, vol. 9, no. 1, p. 1839, May 2018.

[5] B. Nakarmi et al., "Photonically generated frequency hopped linear frequency modulated signal using a DFB laser," *J. Lightw. Technol.*, vol. 40, no. 20, pp. 6729–6736, May 12, 2022.

[6] S.-C. Chan, S.-K. Hwang, and J.-M. Liu, "Period-one oscillation for photonic microwave transmission using an optically injected semiconductor laser," *Opt. Exp.*, vol. 15, no. 22, pp. 14921–14935, Oct. 2007.

[7] H. Chen, P. Zhou, L. Zhang, S. Bassi, B. Nakarmi, and S. Pan, "Reconfigurable identical and complementary chirp dual-LFM signal generation subjected to dual-beam injection in a DFB laser," *J. Lightw. Technol.*, vol. 38, no. 19, pp. 5500–5508, Jul. 15, 2020.

[8] Q. Guo, F. Zhang, P. Zhou, and S. Pan, "Dual-band LFM signal generation by optical frequency quadrupling and polarization multiplexing," *IEEE Photon. Technol. Lett.*, vol. 29, no. 16, pp. 1320–1323, Jun. 30, 2017.

[9] S. Alland, W. Stark, M. Ali, and M. Hegde, "Interference in automotive radar systems: Characteristics, mitigation techniques, and current and future research," *IEEE Signal Process. Mag.*, vol. 36, no. 5, pp. 45–59, Sep. 2019.

[10] S. Lee, J. Lee, and S. Kim, "Mutual interference suppression using wavelet denoising in automotive FMCW radar systems," *IEEE Trans. Intell. Transp. Syst.*, vol. 22, no. 2, pp. 887–897, Feb. 2021.

[11] R. Vignesh, G. A. Shanmugha Sundaram, and K. P. Soman, "Design of less-detectable RADAR waveforms using stepped frequency modulation and coding," *Proc. Comput. Sci.*, vol. 143, pp. 39–47, Jan. 2018.

[12] J. Lachowski, M. Maternia, and J. Górzynski, "Multiband and multicarrier operations in HSDPA," in *Proc. 8th Int. Symp. Wireless Commun. Syst.*, Nov. 2011, pp. 725–729.

[13] Z. Xu, Z. Xie, C. Fan, and X. Huang, "Robust radar waveform design for extended targets with multiple spectral compatibility constraints," *Signal Process.*, vol. 204, Mar. 2023, Art. no. 108850.

[14] L. Li, W. Zhao, X. Su, F. Wu, and B. Fan, "Reconstructing in laser wavelength scanning interference test of aspheric surface," *Proc. SPIE*, vol. 8416, Jun. 2012, Art. no. 841625.

[15] Z. Qin, L. Chen, and X. Bao, "Wavelet denoising method for improving detection performance of distributed vibration sensor," *IEEE Photon. Technol. Lett.*, vol. 24, no. 7, pp. 542–544, Jan. 3, 2012.

[16] M. Kunert, "The EU project MOSARIM: A general overview of project objectives and conducted work," in *Proc. 9th Eur. Radar Conf.*, Nov. 2012, pp. 1–5.

[17] P. Zhou, F. Zhang, Q. Guo, S. Li, and S. Pan, "Reconfigurable radar waveform generation based on an optically injected semiconductor laser," *IEEE J. Sel. Topics Quantum Electron.*, vol. 23, no. 6, pp. 1–9, Nov. 2017.

[18] B. Nakarmi, H. Chen, M. Lee, Y. H. Won, and S. Pan, "Injection with negative wavelength detuning for multispectrum frequency generation and hopping using SMFP-LD," *IEEE Photon. J.*, vol. 9, no. 5, pp. 1–11, Oct. 2017.

[19] Y.-S. Son, H.-K. Sung, and S. Heo, "Automotive frequency modulated continuous wave radar interference reduction using per-vehicle chirp sequences," *Sensors*, vol. 18, no. 9, p. 2831, Aug. 2018.